The First Systematic Synthesis of Heterobimetallic Dithiolene-Bridged Complexes. Synthesis and Characterization of Metal Complexes of 4-(1′,2′-Ethylenedithiolate)-1,3-dithiole-2-one and Dimeric Metal Complexes of 1,2,3,4-Butadienetetrathiolate

Christopher E. Keefer, Suzanne T. Purrington,* Robert D. Bereman,* and Paul D. Boyle

Department of Chemistry, North Carolina State University, Raleigh, North Carolina 27695-8204

Received January 22, 1999

The 1,2-dithiolene ligands 4-(1′,2′-ethylenedithiolate)-1,3-dithiole-2-one ($eddo^{2-}$) and 1,2,3,4-butadienetetrathiolate (bdt^{4-}) are synthesized by the controlled single or double 1,3-dithiole-2-one ring opening of 4,4′-bis(1,3-dithiole-2-one) (bdo) (**1**). The synthesis and characterization of the novel transition metal complexes (COD)Pt(eddo) (**2**), (diphos)Ni(eddo) (**3**), $[Bu_4N][Ni(eddo)_2]$ (**4**), (COD)Pt(bdt)Pt(COD) (**5**), and (diphos)Ni(bdt)Pt(COD) (**6**) (where COD = 1,5-cyclooctadiene, diphos = 1,2-bis(diphenylphosphino)ethane) are reported. Use of $eddo^{2-}$ and bdt^{4-} results in the selective systematic synthesis of transition metal monomers and dimers. In addition, the synthesis of mixed metal dimeric complexes utilizing a "transition metal 1,2-dithiolene" ligand is demonstrated. The single-crystal X-ray structural analyses of the cocrystallized (COD)Pt(eddo)·$^1/_2$bdo, monoclinic, $P2_1/n$, $a = 13.0388(4)$ Å, $b = 9.2048(3)$ Å, $c = 16.2384(5)$ Å, $\beta = 97.289(5)°$, $Z = 4$, and $[Bu_4N][Ni(eddo)_2]$, monoclinic, $P2_1/n$, $a = 8.3508(2)$ Å, $b = 26.4703(7)$, $c = 15.2778(3)$ Å, $\beta = 99.8160(10)°$, $Z = 4$, are reported. There is strong evidence of delocalization through the butadiene backbone of **1** which extends into the sulfur atoms. It also appears that there is some delocalization through the butadiene backbone of the $eddo^{2-}$ ligands in **2** and **4**.

Introduction

Our synthetic interests continue to focus on 1,2-dithiolene ligands and most recently on the development of metal-bridging 1,2-dithiolene ligands where evidence of delocalization exists between the two 1,2-dithiolene groups. Bridging transition metal centers with 1,2-dithiolene ligands can combine the redox behavior of multiple metal centers with the already well-known redox ability of "noninnocent" dithiolene ligands, yielding a number of accessible oxidation states.

The bridging 1,2-dithiolene ligand tetrathiafulvalenetetrathiolate ($TTFS_4^{4-}$) has been reported,[1,2] and several homobimetallic Ti, Ni, and Pt and heterobimetallic Ni−Ti bridged complexes have been studied.[3−6]

Rauchfuss and co-workers have synthesized a dianionic ligand containing a 1,2-dithiolene coordinating group at one end and a 1,1-dithiolene group at the other (Figure 1).[7] The simplest metal-bridging 1,2-dithiolene ligands are $C_2S_4^{n-}$ ($n = 2, 4$). Several researchers have reported metal complexes which contain a bridging $C_2S_4^{n-}$ group, but often only as the consequence of an unexpected reaction unique to special conditions.[8−10] Recently, a systematic approach to homobimetallic transition metal complexes bridged by $C_2S_4^{2-}$ has been developed by Pullen and co-workers.[11−14] Attempts to make use of the reactivity of dithiocarbonate groups for the direct synthesis of metal dimers containing the $C_2S_4^{4-}$ bridging ligand from tetrathiapentalene-2,5-dione (tpd) or 1,3-dithiole-2-oxo-4,5-dithiolate ($dmid^{2-}$) complexes (Figure 2) have not been successful in our laboratories. We have shown recently that the

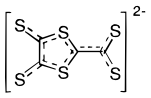

Figure 1. $C_4S_6^{2-}$.

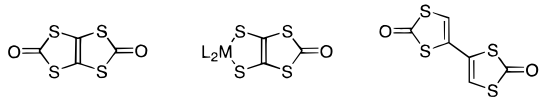

Figure 2. 1,3,4,6-Tetrathiapentalene-2,5-dione (tpd), mono-1,3-dithiole-2-oxo-4,5-dithiolate ($dmid^{2-}$) metal complex, and 4,4′-bis(1,3-dithiole-2-one) (bdo) (**1**).

* To whom correspondence should be addressed.

(1) McCullough, R. D.; Belot, J. A.; Seth, J. *J. Org. Chem.* **1993**, *58*, 6480.
(2) Gemmell, C.; Kilburn, J. D.; Ueck, H.; Underhill, A. E. *Tetrahedron Lett.* **1992**, *33*, 3923.
(3) McCullough, R. D.; Belot, J. A.; Seth, J.; Rheingold, A. L.; Yap, G. P. A.; Cowan, D. O. *J. Mater. Chem.* **1995**, *5*, 1581.
(4) McCullough, R. D.; Belot, J. A.; Rheingold, A. L.; Yap, G. P. A. *J. Am. Chem. Soc.* **1995**, *117*, 9913.
(5) McCullough, R. D.; Belot, J. A. *Chem. Mater.* **1994**, *6*, 1396.
(6) McCullough, R. D.; Seth, J.; Belot, J. A.; Majetich, S. A.; Carter, A. C. *Synth. Met.* **1993**, *55−57*, 1989.
(7) Szczepura, L. F.; Galloway, C. P.; Zheng, Y.; Han, P.; Rheingold, A. L.; Wilson, S. R.; Rauchfuss, T. B. *Angew. Chem., Int. Ed. Engl.* **1995**, *34*, 1890.
(8) Yang, X.; Doxsee, D. D.; Rauchfuss, T. B.; Wilson, S. R. *J. Chem. Soc., Chem. Commun.* **1994**, 821.
(9) Vicente, R.; Ribas, J.; Alvarez, S.; Segui, A.; Solans, X.; Verdaguer, M. *Inorg. Chem.* **1987**, *26*, 4004.
(10) Bianchini, C.; Mealli, C.; Meli, A.; Sabat, M.; Zanello, P. *J. Am. Chem. Soc.* **1987**, *109*, 185.
(11) Pullen, A. E.; Zeltner, S.; Olk, R.-M.; Hoyer, E.; Abboud, K. A.; Reynolds, J. R. *Inorg. Chem.* **1996**, *35*, 4420.
(12) Pullen, A. E.; Abboud, K. A.; Reynolds, J. R.; Piotraschke, J.; Zeltner, S.; Olk, R. M.; Hoyer, E.; Liu, H. L.; Tanner, D. B. *Synth. Met.* **1997**, *86*, 1791.
(13) Pullen, A. E.; Olk, R.-M.; Zeltner, S.; Hoyer, E.; Abboud, K. A.; Reynolds, J. R. *Inorg. Chem.* **1997**, *36*, 958.
(14) Piotraschke, J.; Pullen, A. E.; Abboud, K. A.; Reynolds, J. R. *Inorg. Chem.* **1995**, *34*, 4011.

10.1021/ic990841a CCC: $18.00
Published on Web 11/15/1999

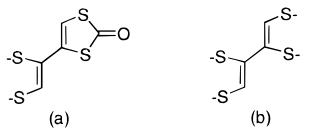

Figure 3. (a) 4-(1′,2′-Ethylenedithiolate)-1,3-dithiole-2-one ($eddo^{2-}$) and (b) 1,2,3,4-butadienetetrathiolate (bdt^{4-}).

tetraanion does not exist in solution,[15] contrary to literature reports.[16]

To further explore the use of compounds with two 1,3-dithiole-2-one groups as precursors to bridging 1,2-dithiolene ligands, we have undertaken a study of the ligands generated from 4,4′-bis(1,3-dithiole-2-one) (bdo) (**1**) (Figure 2). Anderson et al.[17] have reported the synthesis of **1** and its reaction with excess base and nickel acetate to form the neutral nickel bisdithiolene polymer. By developing the appropriate reaction conditions, we have shown that **1** can be used to form the 1,2-dithiolene ligand 4-(1′,2′-ethylenedithiolate)-1,3-dithiole-2-one ($eddo^{2-}$) or the bridging 1,2-dithiolene ligand 1,2,3,4-butadienetetrathiolate (bdt^{4-}) in solution (Figure 3).

In addition, homo- and heterobimetallic complexes of bdt^{4-} can be systematically designed and synthesized from metal complexes of $eddo^{2-}$. Control of the reaction conditions makes possible a wide variety of transition metal complexes, and we report here the synthesis and characterizations of several representative examples: the transition metal mono-1,2-dithiolenes (COD)Pt(eddo) (**2**) and (diphos)Ni(eddo) (**3**), the nickel bisdithiolene $[Bu_4N][Ni(eddo)_2]$ (**4**), the homobimetallic dimer (COD)Pt(bdt)Pt(COD) (**5**), and the heterobimetallic dimer (COD)Pt(bdt)Ni(diphos) (**6**) (COD = 1,5-cyclooctadiene).

Experimental Section

General Procedures. ^{1}H NMR, ^{31}P NMR, and ^{195}Pt NMR were obtained at 300, 121.653, and 64.497 MHz, respectively. All chemical shifts are reported in parts per million downfield of the following references: tetramethylsilane for ^{1}H, external 85% H_3PO_4 in H_2O for ^{31}P, and external 1.0 M Na_2PtCl_6 in D_2O. Melting points are uncorrected. High-resolution mass spectra were obtained on a JEOL HX110HF mass spectrometer using fast atom bombardment (FAB) or electron impact (EI) ionization. Elemental analyses were performed by Atlantic Microlab, Inc., Norcross, GA.

Materials. K_2PtCl_4 (Johnson-Matthey), COD (Matheson), 2,3-butanedione (Acros), 1,2-bis(diphenylphosphino)ethane nickel(II) dichloride ((diphos)$NiCl_2$) (Aldrich), and $NiCl_2{\cdot}6H_2O$ (Aldrich) were used without further purification. 1,5-Cyclooctadiene platinum(II) dichloride ((COD)$PtCl_2$),[18] potassium isopropylxanthate, and 1,4-dibromo-2,3-butanedione[19] were prepared according to literature procedures. All transition metal complex syntheses were carried out under Ar using standard Schlenk techniques.

4,4′-Bis(1,3-dithiole-2-one), bdo (1). To 1,4-dibromo-2,3-butanedione (25.0 g, 0.10 mol) in 500 mL of CH_2Cl_2 was added potassium isopropylxanthate (35.7 g, 0.20 mol) with stirring. After 1 h, the mixture was filtered and the solid washed with CH_2Cl_2 (3 × 100 mL). Longer reaction times resulted in the decomposition of the product and reduced yields. The filtrate and washings were collected, and solvent was removed by evaporation to yield 17.4 g (48%) of the xanthate ester, a dark yellow oil (^{1}H NMR ($CDCl_3$): δ 1.39 (d, 12H, $^3J(^1H-^1H)$ = 6 Hz), 4.33 (s, 4H), 5.66 (septet, 2H, $^1J(^1H-^1H)$ = 6 Hz)). This crude oil was added dropwise to 500 mL of concentrated H_2SO_4 at 0 °C, forming a black solution which was stirred at 0 °C for 5 h and poured onto ~2 L of ice, resulting in a tan precipitate. The mixture was immediately suction filtered, yielding 10.6 g of a tan solid (crude yield 92% from the oil). Recrystallization from ethanol after treatment with activated charcoal gave 10 g (42% overall) of light tan crystals. Mp: 212−215 °C, lit.[17] 214−215 °C. ^{1}H NMR ($CDCl_3$): δ 6.69 (s). ^{1}H NMR (d_6-DMSO): δ 7.46 (s). EI-MS: *m/z* 234 (M^+), 206, 178, 146. Anal. Calcd for $C_6H_2O_2S_4$: C, 30.75; H, 0.86; S, 54.73. Found: C, 30.67; H, 0.84; S, 54.83.

1,5-Cyclooctadiene Platinum(II) 4-(1′,2′-Ethylenedithiolate)-1,3-dithiole-2-one, (COD)Pt(eddo) (2). A solution of NaOEt (0.10 g of Na, 4.4 mmol in 20 mL of ethanol) was cannulated dropwise into **1** (0.47 g, 2.0 mmol) in 100 mL of anhydrous THF. During the addition the color changed from light to dark yellow. After the solution was stirred for 10 min, (COD)$PtCl_2$ (0.75 g, 2.0 mmol) was added all at once. The dark orange solution was stirred overnight and evaporated to dryness. The resulting orange-brown solid was dissolved in a minimal amount of CH_2Cl_2 and chromatographed on a short silica gel column (6 cm × 6 cm) with CH_2Cl_2 as the eluent. The first orange band was collected and evaporated to yield 0.57 g of a yellow-orange solid (56% yield). Mp: 178−180 °C dec. ^{1}H NMR ($CDCl_3$): δ 2.47−2.61 (m, 8H), 5.49 (s with Pt satellites, 2H, $^2J(^1H-^{195}Pt)$ = 53 Hz), 6.56 (s with Pt satellites, 2H, $^1J(^1H-^{195}Pt)$ = 53 Hz), 6.66 (s, 1H), 7.11 (s with Pt satellites, 1H, $^3J(^1H-^{195}Pt)$ = 111 Hz). ^{195}Pt NMR ($CDCl_3$): δ −5331 (s). High-resolution MS (FAB): exact mass calcd for $[C_{13}H_{14}OPtS_4]^+$ (M^+) 508.9597, found 508.9612. Anal. Calcd for $C_{13}H_{14}OPtS_4$: C, 30.64; H, 2.77; S, 25.17. Found: C, 30.70; H, 2.73; S, 25.24.

1,2-Bis(diphenylphosphino)ethane Nickel(II) 4-(1′,2′-Ethylenedithiolate)-1,3-dithiole-2-one, (diphos)Ni(eddo) (3). A solution of NaOEt (0.17 g of Na, 7.6 mmol in 20 mL of ethanol) was cannulated dropwise into **1** (0.89 g, 3.8 mmol) in 200 mL of anhydrous THF. During the addition the color changed from light yellow to dark yellow-brown. After the solution was stirred for 10 min, (diphos)$NiCl_2$ (2.0 g, 3.8 mmol) was added all at once, causing the mixture to turn black. The solution was stirred overnight and evaporated to dryness. The black green solid was dissolved in a minimal amount of CH_2Cl_2 and chromatographed on a silica gel column (7 cm × 30 cm) with CH_2Cl_2 as the eluent. The first blue-green band was collected and evaporated to yield 1.5 g of a forest green solid (60% yield). Mp: 146−150 °C dec. ^{1}H NMR ($CDCl_3$): δ 2.30−2.48 (m, 4H), 6.55 (s, 1H), 6.88 (t, 1H, $^4J(^1H-^{31}P)$ = 3 Hz), 7.44−7.55 (m, 12H), 7.77 (d of t, 8H, $^4J(^{13}C-^{31}P)$ = 9 Hz, $^3J(^{13}C-^1H)$ = 8 Hz). ^{31}P{^{1}H} NMR ($CDCl_3$): δ 58.4. FAB-MS: *m/z* 662 (M^+). Anal. Calcd for $C_{31}H_{26}OP_2NiS_4{\cdot}H_2O$: C, 54.64; H, 4.14; S, 18.82. Found: C, 54.91; H, 4.03; S, 18.79.

Tetra(*n*-butyl)ammonium Nickel(II) Bis(4-(1′,2′-ethylenedithiolate)-1,3-dithiole-2-one), $[Bu_4N][Ni(eddo)_2]$ (4). 1 (0.50 g, 2.1 mmol) was added to NaOEt (0.11 g of Na, 4.8 mmol in 20 mL of ethanol) and stirred for 30 min. The dark yellow solution was cannulated dropwise into $NiCl_2{\cdot}6H_2O$ (0.25 g, 1.1 mmol in 300 mL of ethanol). During the addition, the color changed from a light yellow-green to a very dark red-brown. The solution was stirred for 1 h and was exposed to air for the last 15 min to facilitate oxidation. Tetra(*n*-butyl)ammonium bromide (0.34 g, 1.1 mmol) was added all at once and the solution stirred for 30 min before extraction with H_2O/CH_2Cl_2. The organic layer was collected and dried with $MgSO_4$. To the CH_2Cl_2 solution (500 mL) was added ca. 400 mL of diethyl ether, and the solution was cooled at −28 °C overnight. A microcrystalline dark red-brown precipitate (0.45 g) was filtered from the solution (56% yield). Mp: 163−164 °C. High-resolution MS (FAB): exact mass calcd for $[C_{10}H_4NiO_2S_8]^+$ ($M - (Bu_4N))^-$ 469.7331, found 469.7375. Anal. Calcd for $C_{26}H_{40}NNiO_2S_8$: C, 43.75; H, 5.65; N, 1.96; S, 35.94. Found: C, 43.58; H, 5.69; N, 1.94; S, 35.72.

Bis(1,5-cyclooctadiene platinum(II)) 1,2,3,4-Butadienetetrathiolate, (COD)Pt(bdt)Pt(COD) (5). A solution of NaOEt (0.10 g of Na, 4.3 mmol in 20 mL of ethanol) was cannulated dropwise into **1** (0.25 g, 1.1 mmol in 200 mL of anhydrous THF). During the addition the color changed from light yellow to dark red. The solution was stirred for 30 min, and (COD)$PtCl_2$ (0.80 g, 2.1 mmol in 100 mL of anhydrous THF) was added all at once, causing the mixture to turn dark orange.

(15) Keefer, C. E.; Purrington, S. T.; Bereman, R. D. *Synthesis* **1998**, 1710.
(16) Vicente, R.; Ribas, J.; Cassoux, P.; Valade, L. *Synth. Met.* **1986**, *13*, 265.
(17) Andersen, J. R.; Patel, V. V.; Engler, E. M. *Tetrahedron Lett.* **1978**, 239.
(18) McDermott, J. X.; White, J. F.; Whitesides, G. M. *J. Am. Chem. Soc.* **1976**, *98*, 6521.
(19) Ruggli, P.; Herzog, M.; Wegmann, J.; Dahn, H. *Helv. Chim. Acta* **1946**, *29*, 95.

The solution was stirred overnight and evaporated to dryness. The resulting orange-brown solid was dissolved in a minimal amount of CH_2Cl_2 and chromatographed on a silica gel column (7 cm × 25 cm) with CH_2Cl_2 as the eluent. The first orange band was collected and evaporated to yield 0.79 g of a yellow-orange solid (48% yield). Mp: 220−230 °C dec. ^{1}H NMR ($CDCl_3$): δ 2.48−2.57 (m, 16H), 5.42 (s with Pt satellites, 4H, $^2J(^1H-^{195}Pt) = 53$ Hz), 5.51 (s with Pt satellites, 4H, $^1J(^1H-^{195}Pt) = 54$ Hz), 7.21 (s with Pt satellites, 1H, $^3J(^1H-^{195}Pt) = 114$ Hz). High-resolution MS (FAB): exact mass calcd for $[C_{20}H_{26}Pt_2S_4]^+$ (M^+) 784.8504, found 784.0237. Anal. Calcd for $C_{20}H_{26}Pt_2S_4$: C, 30.61; H, 3.34; S, 16.34. Found: C, 30.65; H, 3.31; S, 16.45.

1,5-Cyclooctadiene Platinum(II) 1,2,3,4-Butadienetetrathiolate Nickel(II) 1,2-Bis(diphenylphosphino)ethane, (COD)Pt(bdt)Ni(diphos) (6). A solution of NaOEt (0.035 g of Na, 1.5 mmol in 10 mL of ethanol) was cannulated dropwise into **3** (0.50 g, 0.75 mmol in 150 mL of anhydrous THF). During the addition the color changed from blue-green to brown. The solution was stirred for 30 min, and (COD)$PtCl_2$ (0.28 g, 0.75 mmol in 100 mL of anhydrous THF) was added all at once. The solution was stirred overnight and evaporated to dryness. The resulting brown solid was dissolved in a minimal amount of 1,2-dichloroethane and chromatographed on a silica gel column (7 cm × 30 cm) with 1,2-dichloroethane as the eluent. The third colored band (yellow-green) was collected and evaporated to yield 0.22 g of a yellow-green solid (31% yield). Mp: 120 °C dec. ^{1}H NMR ($CDCl_3$): δ 2.29−2.51 (m, 12H), 5.32 (s with Pt satellites, 2H, $^2J(^1H-^{195}Pt) = 56$ Hz), 5.42 (s with Pt satellites, 2H, $^2J(^1H-^{195}Pt) = 51$ Hz), 7.00 (s, 1H), 7.12 (s with Pt satellites, 1H, $^3J(^1H-^{195}Pt) = 120$ Hz), 7.42−7.53 (m, 12H), 7.78−7.80 (m, 8H). High-resolution MS (FAB): exact mass calcd for $[C_{38}H_{38}NiP_2PtS_4]^+$ (M^+) 937.0333, found 937.0365. Anal. Calcd for $C_{38}H_{38}NiP_2PtS_4 \cdot CH_2ClCH_2Cl$: C, 46.30; H, 4.08; S, 12.36. Found: C, 45.94; H, 4.03; S, 12.80.

Crystal Structure Determinations. Compounds **1** and **2** were cocrystallized from a chloroform solution, yielding an orange needlelike crystal which was mounted on the end of glass fibers using 5 min epoxy. All X-ray measurements were made on an Enraf-Nonius CAD4 diffractometer. The unit cell dimensions were determined by a symmetry-constrained fit of 24 well-centered reflections, and their Friedel pairs were measured at $\pm\theta$ values with $39° < 2\theta < 45°$. A quadrant of intensity data was collected using the $\theta/2\theta$ scan mode at room temperature. Three standard reflections were measured every 4800 s of X-ray exposure time. The crystal orientation was checked every 400 reflections. Scaling the data was accomplished using a five-point smoothed curved routine fit to the intensity check reflections. The intensity data were corrected for Lorentz and polarization effects. An empirical absorption correction was performed using ψ scan data from three reflections. The data were reduced, and graphics were produced using routines from the NRCVAX[20] set of programs. The structure was solved by direct methods using SIR92.[21] Most of the non-H atomic positions of the Pt-containing molecule were recovered from the initial E-map. The remaining atomic positions were recovered from subsequent difference Fourier syntheses. The calculated structure factors were fit to the data using full matrix least-squares based on *F*. All non-H atoms were allowed to refine with anisotropic displacement parameters (ADPs). The hydrogen atoms were included in the structure factor calculation but not refined. Carbon−hydrogen distances were set to 0.96 Å, and the isotropic displacements (U(H)) were set according to the expression $U(H) = U(C) + 0.01$ Å^2. The hydrogen positional and displacement parameters were updated after every other cycle of least squares. The calculated structure factors included corrections for anomalous dispersion from the usual tabulation.[22] In the final refinement, a secondary extinction correction was included.

Compound **4** was crystallized from the vapor diffusion of diethyl ether into a chloroform solution of the dark red salt, yielding a gray platelike crystal. Refinement on F^2 was performed for all reflections except for 26 with very negative F^2 or flagged by the user for potential systematic errors. Weighted *R* factors R_w and all goodnesses of fit *S* are based on F^2; conventional *R* factors *R* are based on *F*, with *F* set to zero for negative F^2. The observed criterion of $F^2 > 2\sigma(F^2)$ is used only for calculating the *R* factor and is not relevant to the choice of reflections for refinement. *R* factors based on F^2 are statistically approximately twice as large as those based on *F*, and *R* factors based on all data will be even larger. Crystallographic parameters are given in Table 1 for both structures.

Table 1. Single-Crystal X-ray Analysis Parameters for (COD)Pt(eddo)·$^1/_2$bdo and $[Bu_4N][Ni(eddo)_2]$ (**4**)

	2·$^1/_2$**1**	**4**
empirical formula	$C_{16}H_{15}O_2PtS_6$	$C_{26}H_{40}NNiO_2S_8$
fw	626.74	713.78
cryst dimens (mm)	0.40 × 0.16 × 0.04	0.02 × 0.20 × 0.38
temp (K)	298	158
cryst syst	monoclinic	monoclinic
space group	$P2_1/n$ (no. 14)	$P2_1/n$ (no. 14)
a (Å)	13.0388(4)	8.3508(2)
b (Å)	9.2048(3)	26.4703(7)
c (Å)	16.2384(5)	15.2778(3)
β (deg)	97.289(5)	99.8160(10)
V (Å^3)	1933.18(10)	3327.69(14)
Z	4	4
ρ_{calcd} (g cm^{-3})	2.153	1.425
μ (cm^{-1})	7.97	0.1110
R_F, R_{wF}[a]	0.035, 0.046	0.0834, 0.1948 (F_o^2)

[a] $R_F = \sum(|F_o - F_c|)/\sum F_o$, $R_{wF} = [\sum w(|F_o - F_c|)^2/\sum wF_o^2]^{1/2}$, where $w = [\sigma^2(F) + gF^2]^{-1}$.

A gray plate of dimensions 0.38 × 0.20 × 0.02 mm was mounted on a standard Siemens SMART CCD-based X-ray diffractometer equipped with an LT-2 low-temperature device and a normal focus Mo target X-ray tube ($\lambda = 0.710\ 73$ Å) operated at 2000 W power (50 kV, 40 mA). The X-ray intensities were measured at 158 K; the detector was placed at a distance of 5.103 cm from the crystal. A full sphere of data consisting of a total of 2132 frames were collected with a scan width of 0.38 in ω and an exposure time of 90 s/frame. The frames were integrated with the Siemens SAINT software package using a narrow frame algorithm. The integration of the data using a primitive monoclinic unit cell yielded a total of 30 721 reflections to a maximum 2θ value of 49.6°, 5832 of which were independent and 4013 of which were greater that $2\sigma(I)$. The final cell constants (Table 1) were based on the centroids of 5638 reflections above $10\sigma(I)$. Analysis of the data showed negligible decay during data collection; the data were corrected for absorption using an empirical method (SADABS) with transmission coefficients ranging from 0.532 to 1.065. The structure was solved and refined with the Siemens SHELXTL (version 5.03) software package, using the space group $P2_1/n$ with $Z = 4$ for the formula $C_{26}H_{40}NO_2S_8Ni$. All non-hydrogen atoms were refined anisotropically, with the hydrogen atoms placed in idealized positions with common isotropic thermal parameters. The final full matrix refinement based on F^2 converged at $R = 0.0834$ and $R_w^2 = 0.1948$ (based on observed data) and $R = 0.1201$ and $R_w^2 = 0.2167$ (based on all data). The largest peak/hole in the final difference Fourier map is +1.483/−0.961 e Å^{-3}.

Results and Discussion

Synthesis. The ligand precursor bdo (**1**) was synthesized according to a variation of the literature procedure[17] as shown in Scheme 1. It is important to note that extended reaction times for the reaction of 1,4-dibromo-2,3-butanedione with potassium isopropylxanthate resulted in significant decomposition of the product. It is recommended that the reaction time be no longer than 1 h. In addition, the use of acetone, similar to previously reported xanthate addition reactions,[23,24] instead of methylene chloride as a solvent, results in immediate decomposition of

(20) Gabe, E. J.; Le Page, Y.; Charland, J.-P.; Lee, F. L.; White, P. S. *J. Appl. Crystallogr.* **1989**, *22*, 384.
(21) Altomare, A.; Burla, M. C.; Camalli, G.; Cascarano, G.; Giacovazzo, C.; Guagliardi, A.; Polidori, G. *J. Appl. Crystallogr.* **1994**, *27*, 435.
(22) *International Tables for X-ray Crystallography*; Kynoch Press: Birmingham, England, 1974; Vol. IV.
(23) Schumaker, R. R.; Engler, E. M. *J. Am. Chem. Soc.* **1977**, *99*, 5521.
(24) Larsen, J.; Lenoir, C. *Org. Synth.* **1993**, *72*, 265.

Scheme 1

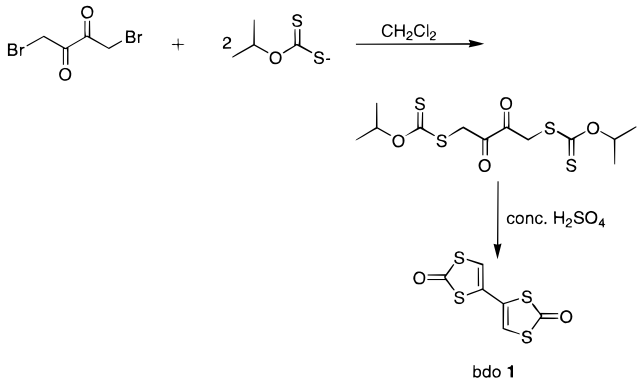

Scheme 2

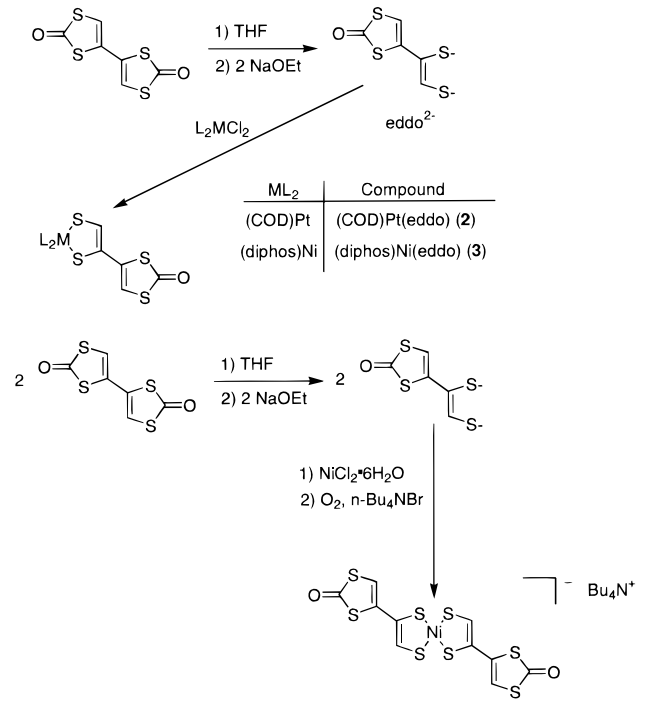

the mixture. Prompt workup is required after the addition of the concentrated H_2SO_4 solution to ice as decomposition was observed after standing.

Reaction of **1** with 2 equiv of an alkoxide results in an opening of one 1,3-dithiole-2-one ring, yielding the yellow 1,2-dithiolene ligand in solution (Scheme 2). The reaction must be performed under conditions which minimize the formation of the doubly-ring-opened product bdt^{4-}. Dissolving bdo in THF and then adding the alkoxide dropwise is effective in suppressing the second ring-opening reaction. To obtain the dark red bdt^{4-} anion in solution, reaction of 4 equiv of alkoxide base with **1** is required. The drastic difference in color provides a convenient way to distinguish between the two anions in solution.

Compounds **2**, **3**, and **4** were synthesized according to Scheme 2. Like other nickel bis(1,2-dithiolenes), the intermediate to **4** underwent air oxidation to the monoanion. The homobimetallic compound **5** was synthesized directly from the bdt^{4-} ligand and 2 equiv of $(COD)PtCl_2$ as shown in Scheme 3. The heterobimetallic compound **6** was synthesized from **3** according to Scheme 3. This last reaction demonstrates the synthetic flexibility of these compounds since the 1,3-dithiole-2-one group is still susceptible to attack by base to form the 1,2-dithiolene intermediate even though it is coordinated to a metal. This

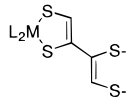

Figure 4. "Transition metal 1,2-dithiolene" ligand.

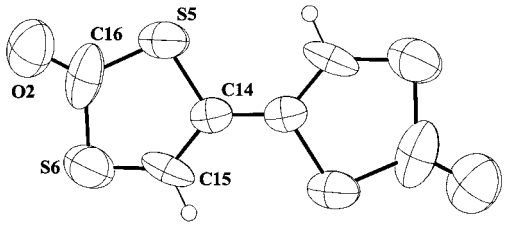

Figure 5. Molecular structure and atom labeling scheme for bdo (**1**). ADP ellipsoids drawn at the 50% probability level. Hydrogens set to arbitrary radii for clarity.

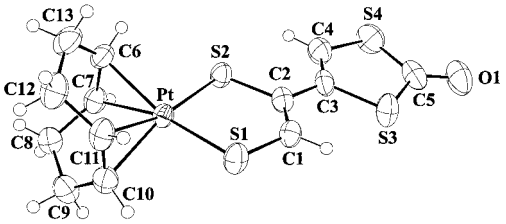

Figure 6. Molecular structure and atom labeling scheme for (COD)Pt(eddo) (**2**). ADP ellipsoids drawn at the 50% probability level. Hydrogens set to arbitrary radii for clarity.

Scheme 3

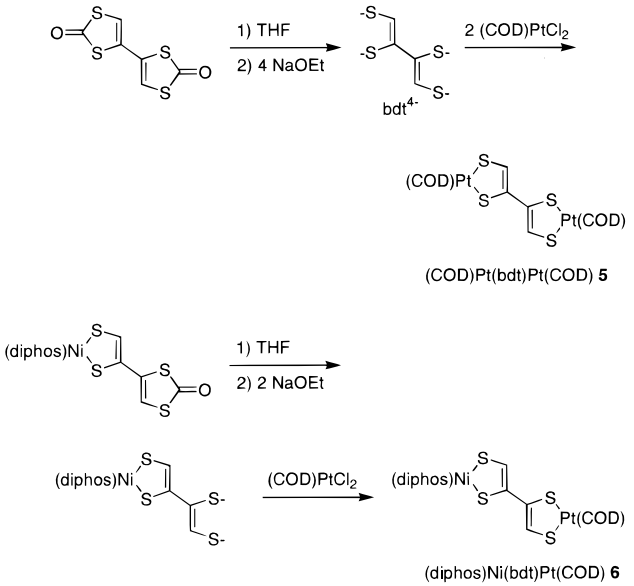

"metal 1,2-dithiolene" ligand (Figure 4) can then react with various transition metals. A wide range of dimeric and oligomeric metal complexes may be potentially synthesized in this fashion.

X-ray Structural Analyses. Slow evaporation of a chloroform solution of (COD)Pt(eddo) (**2**) and bdo (**1**) yielded a single crystal suitable for X-ray structural analysis. Analysis showed that **2** and **1** cocrystallized in a 2:1 ratio. Figures 5 and 6 show ORTEP diagrams and atom labeling for **1** and **2**, respectively. Bond lengths and angles are given in Tables 2 and 3. Figure 7 shows the unit cell and orientation of the molecules. The fortuitous cocrystallization made possible a careful comparison of the structural characteristics of both bdo and the coordinated $eddo^{2-}$ ligand.

Table 2. Selected Bond Lengths (Å) and Bond Angles (deg) for bdo (**1**)

		Bond Lengths			
C14−C15	1.385(10)	S6−C15	1.579(11)	S6−C16	1.811(14)
C14−C14a	1.450(15)	S5−C16	1.731(12)	O2−C16	1.207(13)
S5−C14	1.740(7)				
		Bond Angles			
C14a−C14−C15	130.3(7)	S6−C15−C14	127.6(7)	S5−C16−S6	112.4(5)
S5−C14−C14a	120.6(5)	C14−S5−C16	97.9(5)	S5−C16−O2	128.6(11)
S5−C14−C15	109.1(6)	C15−S6−C16	93.0(4)		

Table 3. Selected Bond Lengths (Å) and Bond Angles (deg) for (COD)Pt(eddo) (**2**)

		Bond Lengths			
Pt−S1	2.2713(15)	C1−C2	1.336(8)	C6−C7	1.376(8)
Pt−S2	2.2740(13)	C2−C3	1.485(8)	C10−C11	1.407(9)
Pt−C6	2.200(6)	C3−C4	1.329(9)	C7−C8	1.546(8)
Pt−C7	2.216(6)	S3−C3	1.761(6)	C6−C13	1.520(9)
Pt−C10	2.203(5)	S4−C4	1.731(7)	C9−C10	1.505(9)
Pt−C11	2.208(5)	S3−C5	1.749(7)	C11−C12	1.504(10)
S1−C1	1.734(6)	S4−C5	1.763(9)	C8−C9	1.510(9)
S2−C2	1.752(6)	O1−C5	1.222(9)	C12−C13	1.550(10)
		Bond Angles			
S1−Pt−S2	88.91(5)	C6−Pt−C10	96.82(22)	S3−C3−C2	117.9(4)
S1−Pt−C10	90.31(16)	C7−Pt−C11	87.96(21)	S3−C3−C4	115.6(5)
S1−Pt−C11	93.75(17)	Pt−S1−C1	103.75(20)	S4−C4−C3	118.9(5)
S2−Pt−C6	90.33(15)	Pt−S2−C2	103.31(19)	C3−S3−C5	96.6(3)
S2−Pt−C7	94.56(15)	S1−C1−C2	122.2(4)	C4−S4−C5	95.9(3)
C6−Pt−C7	36.32(22)	S2−C2−C1	121.7(4)	S3−C5−S4	112.8(4)
C10−Pt−C11	37.21(24)	S2−C2−C3	115.5(4)	S3−C5−O1	123.6(7)
C7−Pt−C10	80.78(22)	C1−C2−C3	122.8(5)	S4−C5−O1	123.5(6)
C6−Pt−C11	81.49(22)	C2−C3−C4	126.5(6)		

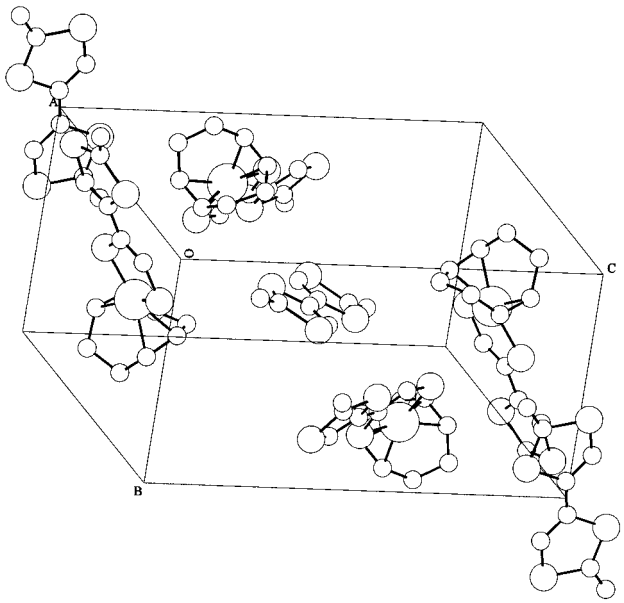

Figure 7. PLUTO[20] unit cell diagram for (COD)Pt(eddo)·$^1/_2$bdo. Hydrogens omitted for clarity.

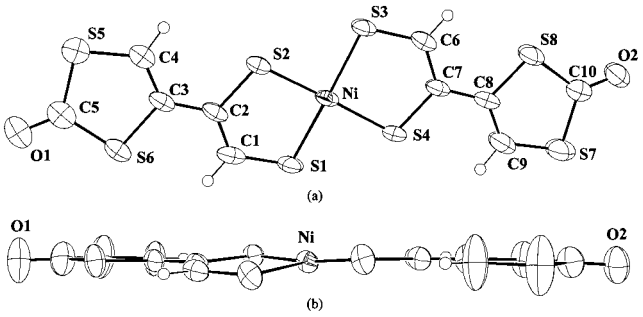

Figure 8. (a) Molecular structure and atom labeling scheme for [Bu_4N][Ni(eddo)$_2$] (**4**). ADP ellipsoids drawn at the 50% probability level. Hydrogens set to arbitrary radii for clarity. (b) Side view showing the twist of the five-membered ring containing Ni, C1, C2, S1, and S2.

For **1**, the molecule sits on a crystallographic center of symmetry and is planar with a dihedral angle between the two five-membered rings of 0.0(3)°. The C14−C15 double bonds adopt an *s-trans* conformation about the C14−C14a single bond, similar to the behavior of 1,3-butadiene. The C14−C15 double bond length (1.38(1) Å) and C14−C14a single bond length (1.45(1) Å) are also similar to those of 1,3-butadiene (1.37 and 1.46 Å). These bond lengths are consistent with modest delocalization of π density across the C14−C14a bond. In addition, the S6−C15 bond length of 1.58(1) Å is significantly shorter than typical C−S single bond lengths (1.70−1.80 Å). As a comparison, a search of the Cambridge Crystallographic Database[25] for all compounds containing a 1,3-dithiole-2-one ring showed that C(C═C double bond)−S bond lengths range from 1.72 Å[26] to 1.76 Å,[27] indicating that the delocalization in **1** extends into the S6 atoms. In contrast, the C14−S5 bond length (1.74(1) Å) is similar to other previously reported C(C═C double bond)−S bonds, showing that S5 is not delocalized through the 1,3-butadiene backbone.

For **2**, the eddo^{2-} ligand is essentially planar with a dihedral angle between the two five-membered rings of 4.4(1)°. Similar to those of **1**, the C1═C2 and C3═C4 double bonds have adopted an *s-trans* conformation about the C2−C3 single bond. These observations are consistent with delocalization within the C1−C2−C3−C4 backbone. However, evidence for delocalization into S1 and S4 is not as clear in the eddo ligand. The C1−S1 (1.73(1) Å), C2−S2 (1.75(1) Å), C3−S3 (1.76(1) Å), and C4−S4 (1.73(1) Å) bond lengths are in the range of similar C−S bonds. Pt−S (2.271(1) and 2.274(1) Å), Pt−C (2.21 Å

(25) Allen, F. H.; Kennard, O. *Chem. Des. Automat. News* **1993**, *8*, 31.
(26) Watson, W. H.; Eduok, E. E.; Kashyap, R. P.; Krawiec, M. *Tetrahedron* **1993**, *49*, 3035.
(27) Sun, S. Q.; Zhang, B.; Wu, P. J.; Zhu, D. B. *J. Chem. Soc., Dalton Trans.* **1997**, 277.

Table 4. Selected Bond Lengths (Å) and Bond Angles (deg) for $[Bu_4N][Ni(eddo)_2]$ (**4**)

		Bond Lengths			
Ni−S1	2.147(2)	S5−C4	1.732(9)	C1−C2	1.347(10)
Ni−S2	2.147(2)	S5−C5	1.762(9)	C2−C3	1.466(10)
Ni−S3	2.154(2)	S6−C3	1.752(7)	C3−C4	1.332(11)
Ni−S4	2.143(2)	S6−C5	1.774(10)	C5−O1	1.208(10)
S1−C1	1.687(8)	S7−C9	1.732(10)	C6−C7	1.361(9)
S2−C2	1.739(6)	S7−C10	1.762(8)	C7−C8	1.457(11)
S3−C6	1.712(8)	S8−C8	1.738(7)	C8−C9	1.329(12)
S4−C7	1.726(7)	S8−C10	1.765(8)	C10−O2	1.189(9)
		Bond Angles			
S4−Ni−S1	87.97(8)	C3−S6−C5	97.1(4)	S5−C5−S6	111.9(5)
S4−Ni−S2	173.49(8)	C8−S8−C10	98.8(4)	C7−C6−S3	121.3(5)
S1−Ni−S2	91.60(8)	C2−C1−S1	122.1(6)	C6−C7−C8	123.3(6)
S4−Ni−S3	91.59(8)	C1−C2−C3	123.7(6)	C6−C7−S4	118.7(6)
S1−Ni−S3	172.21(8)	C1−C2−S2	118.6(6)	C8−C7−S4	118.0(5)
S2−Ni−S3	89.70(7)	C3−C2−S2	117.6(5)	C9−C8−C7	126.6(7)
C1−S1−Ni	103.9(2)	C4−C3−C2	126.2(6)	C9−C8−S8	113.9(7)
C2−S2−Ni	103.7(3)	C4−C3−S6	115.4(6)	C7−C8−S8	119.3(5)
C6−S3−Ni	103.7(2)	C2−C3−S6	118.4(5)	C8−C9−S7	120.2(7)
C7−S4−Ni	104.7(3)	C3−C4−S5	119.2(6)	O2−C10−S7	124.3(6)
C4−S5−C5	96.3(4)	O1−C5−S5	124.5(8)	O2−C10−S8	124.6(6)
C9−S7−C10	96.2(4)	O1−C5−S6	123.5(8)	S7−C10−S8	110.9(5)

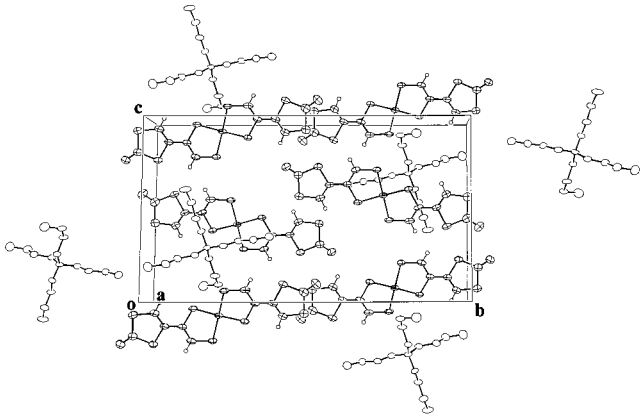

Figure 9. Unit cell diagram for $[Bu_4N][Ni(eddo)_2]$ (**4**). ADP ellipsoids drawn at the 50% probability level. Hydrogens omitted from tetrabutylammonium cations for clarity. Hydrogens set to arbitrary radii for the $Ni(eddo)_2$ anion for clarity.

av), and internal COD bond lengths are similar to those of other previously reported (COD)Pt(1,2-dithiolenes).[28]

In $[Bu_4N][Ni(eddo)_2]$ (**4**), both eddo ligands are again *s-trans*, similar to those of **2**. The ORTEP diagram and atom labeling scheme of the $Ni(eddo)_2$ anion are shown in Figure 8a, and a unit cell packing diagram is given in Figure 9. The five-membered rings in each of the eddo ligands are essentially planar with a maximum mean deviation from the planes of 0.0154 Å. There is a slight twisting of the five-membered ring containing Ni, C1, C2, S1, and S2 out of the plane containing the other three five-membered rings (Figure 8b). This results in nonplanarity of the NiS_4 core with a dihedral angle between the two five-membered rings containing the Ni atom of 9.7°. The ligands in this structure are also in a "*trans*" configuration about the metal center with respect to the two terminal 1,3-dithiole-2-one rings. The Ni−S bond lengths are essentially the same with an average of 2.148(2) Å and are similar to other Ni−S bond lengths in nickel bisdithiolene monoanions.[29] Analysis of the C−S bond lengths in the two ligands shows that the C1−S1 bond (1.687(8) Å) is somewhat shorter than the C2−S2 bond (1.739(6) Å) similar to those of the precursor bdo (**1**). However, the C6−S3 and C7−S4 bonds (1.712(8) and 1.726(7) Å) are essentially the same. The C−C bond lengths of the butadiene backbone in the eddo ligands of **4** are similar to those of **2** (Tables 3 and 4). It appears that the delocalization of the butadiene backbone may extend somewhat into the terminal thiolates of eddo in **4** on the basis of the intermediate nature of the bond lengths.

Conclusion

We have reported the initial synthesis and characterization of several transition metal complexes involving the 1,2-dithiolene ligand $eddo^{2-}$ and the bridging 1,2-dithiolene ligand $bdt.^{4-}$ The synthetic schemes presented demonstrate that controlled opening of the 1,3-dithiole-2-one rings of bdo makes possible a wide variety of transition metal monomers, dimers, and oligomers. In addition, unlike $dmid^{2-}$, $eddo^{2-}$ is susceptible to alkoxide attack even while coordinated to a transition metal. This reactivity makes possible very controlled syntheses of bdt^{4-}-bridged complexes. To our knowledge, this is the first example of a systematic synthetic route to a wide range of heterobimetallic complexes bridged by a 1,2-dithiolene ligand. The planarity and *s-trans* conformation of the eddo ligand suggest that bdt^{4-} should be an effective electronic bridge between metal centers with a conjugated π system.

Acknowledgment. We gratefully acknowledge Johnson-Matthey for a generous loan of K_2PtCl_4 and the National Science Foundation (NSF) (Grant CHE-9509532) for the purchase of the X-ray diffractometer. Mass spectra were obtained at the Mass Spectrometry Laboratory for Biotechnology at North Carolina State University. Partial funding for the facility was obtained from the North Carolina Biotechnology Center and the NSF. We also thank Jeff Kampf at the University of Michigan for performing the single-crystal X-ray crystallographic analysis of **4**.

Supporting Information Available: X-ray crystallographic files in CIF format for complexes $\mathbf{2}\cdot{}^1/_2\mathbf{1}$ and **4**. This material is available free of charge via the Internet at http://pubs.acs.org.

IC990841A

(28) Keefer, C. E.; Purrington, S. T.; Bereman, R. D.; Knight, B. W.; Bedgood Jr., D. R.; Boyle, P. D. *Inorg. Chim. Acta*, in press.
(29) Welch, J.-H.; Bereman, R. D.; Singh, P.; Haase, D.; Hatfield, W. E.; Kirk, M. L. *Inorg. Chim. Acta* **1989**, *162*, 89.